

### 3D Coffee Stain

Itir Bakis Dogru<sup>1</sup>, Cagla Kosak Soz<sup>2,5</sup>, Daniel Aaron Press<sup>3</sup>, Rustamzhon Melikov<sup>3</sup>, Efe Begar<sup>4</sup>, Deniz Conkar<sup>4</sup>, Elif Nur Firat Karalar<sup>4</sup>, Emel Yilgor<sup>2,5</sup>, Iskender Yilgor<sup>1,2,5</sup> and Sedat Nizamoglu<sup>1,3,5,\*</sup>

<sup>1</sup>Graduate School of Biomedical Sciences and Engineering, <sup>2</sup>Department of Chemistry, <sup>3</sup>Department of Electrical and Electronics Engineering, <sup>4</sup>Department of Molecular Biology and Genetics, <sup>5</sup>KUYTAM Surface Science and Technology Research Center  
Koc University, Sariyer, Istanbul, 34450 Turkey

## ATR-IR Investigation

ATR-IR is a useful technique in determining the presence and the extent of possible inter- and/or intramolecular interactions in silk because the changes in crystallinity and H-bonding can easily be detected by comparing the peak shift and intensity changes in the spectra of amorphous and crystalline samples, especially by interpreting the 1400-1800  $\text{cm}^{-1}$  region (amide I and amide II region) in FTIR spectra.

ATR-IR spectra of 3 different silk fibroin samples were investigated in this study. First sample is the silk fibroin film prepared by spin-coating of silk fibroin solution onto glass slide and evaporating the water. Second sample, methanol treated film, is prepared by dipping of spin-coated silk fibroin film into methanol. Third sample is the 3D silk fibroin sphere obtained by evaporating water in pendant droplet. ATR-IR spectra of these samples are provided in Fig. S1.

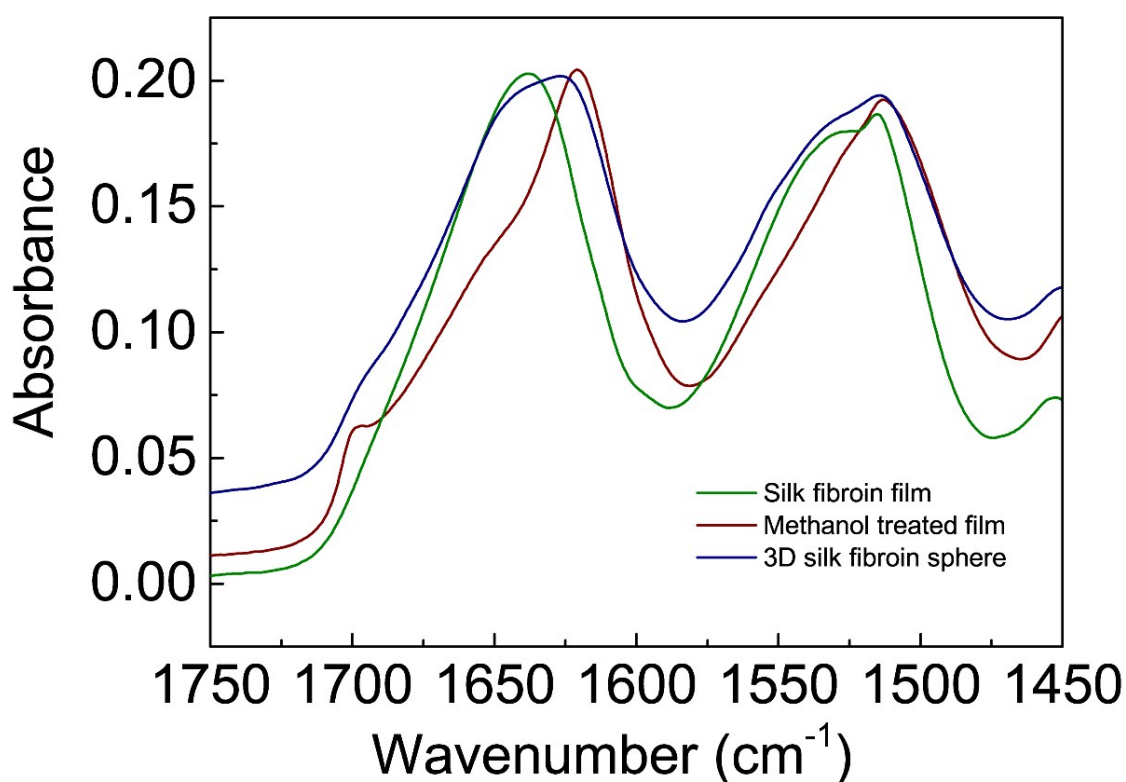


**Fig. S1.** ATR-IR spectra of amide I and amide II regions for silk fibroin samples.

The amide group of silk has characteristic vibrational modes (amide modes) which are sensitive to the protein conformation [1]. Amide I peak of silk fibroin is in 1640-1660  $\text{cm}^{-1}$  region, which splits into two peaks at around 1620 and 1650  $\text{cm}^{-1}$  upon crystallization of fibroin resulting in  $\beta$ -sheet structure. Also, a shoulder at 1690-1700  $\text{cm}^{-1}$  region appears. Amide II peak is at 1540-1535  $\text{cm}^{-1}$ . A shift of this peak to lower wavenumbers is observed upon  $\beta$ -sheet formation due to increased H-bonding between N-H and C=O of amide group [2-4]. Furthermore, vibrations of certain amino-acid side chains have absorption bands in the 1480–1350  $\text{cm}^{-1}$  region (not shown) and may contribute to the intensity of characteristic protein amide bands [1].

Silk fibroin film shows amide I and II peaks at 1638, 1531, and 1513  $\text{cm}^{-1}$ , respectively. This indicates that the silk fibroins are mainly found in an amorphous,  $\alpha$ -helical state with some crystallization. On the other hand, methanol treated silk fibroin is found in  $\beta$ -sheet conformation since amide I absorption is observed as a sharp peak at 1620 and shoulders at 1651 and 1699  $\text{cm}^{-1}$ . Amide II peak of methanol treated silk fibroin has the highest magnitude of shift and is located at 1513  $\text{cm}^{-1}$ . Silk fibroin sphere has amide I peaks at around 1626  $\text{cm}^{-1}$  and 1646  $\text{cm}^{-1}$  and a slight shoulder at 1695  $\text{cm}^{-1}$ , indicating that the compound has slight  $\beta$ -sheet formation. Amide II peak of this sample is at 1513  $\text{cm}^{-1}$  with a shoulder around 1531  $\text{cm}^{-1}$ . Therefore, it can be concluded that the silk fibroin sphere is more crystalline than the spin-coated silk fibroin film.

Polymer crystallization from solution is a time and temperature dependent process. Since spin coating is a very fast process polymer chains will not have enough time to organize/pack or reach their maximum crystallinity. In addition during spin coating due to the fast evaporation of solvent the temperature will also drop, which will also hinder crystallization. On the other hand droplet evaporation is very slow, which allows the polymer chains to pack well and achieve higher crystallization resulting in a robust and stable dome.

Fig. S2 shows that 3D coffee stain can be obtained using aqueous solutions of synthetic polymers, such as polyvinylpyrrolidone and polyvinylalcohol.

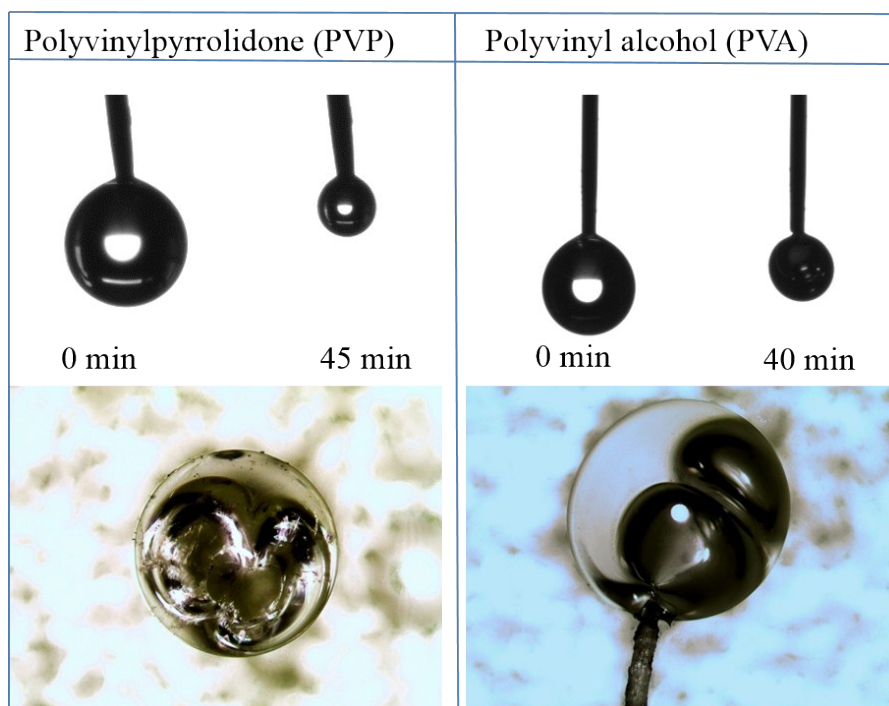


**Fig. S2** Images of 3D coffee stain from polyvinylpyrrolidone and polyvinylalcohol.

Superhydrophobic surfaces are produced by the introduction of silica particles (1 to 10  $\mu\text{m}$  in size) which are randomly distributed on the polymer surface as added in the Fig. S3. This may result in the distortion of the contact area and the wetting.

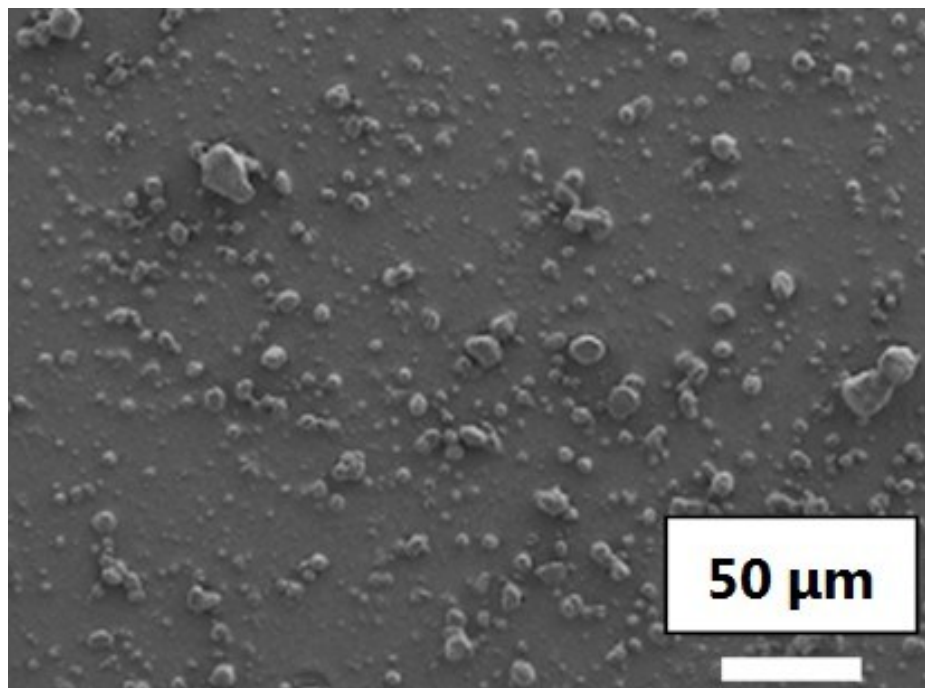
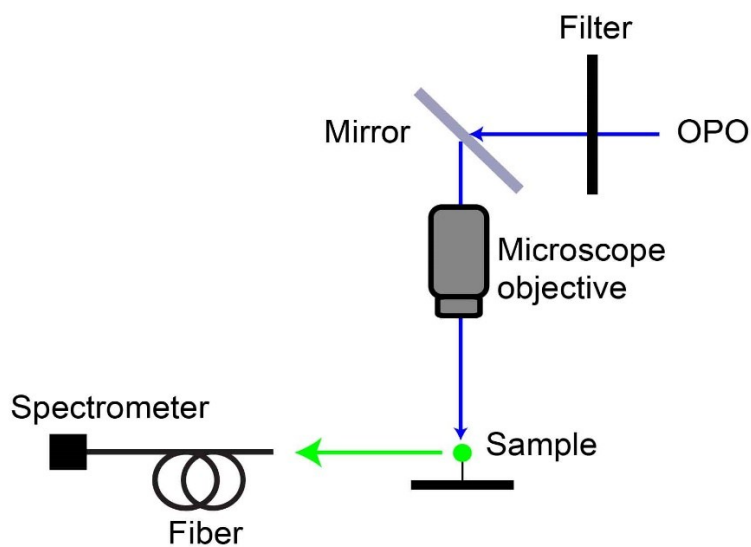


Fig. S3 Superhydrophobic polydimethylsiloxane-urea (SHPSU) surface.

Fig. S4 describes the schematic view of the optical set-up used in protein laser experiments.



**Fig. S4** Schematic view of the optical set-up.

## References

1. Emilia Bramantia, D.C., Claudia Forte, Mario Giovanneschi, Massimo Masetti, Carlo Alberto Veracini, *Solid state  $^{13}\text{C}$  NMR and FT-IR spectroscopy of the cocoon silk of two common spiders*. *Spectrochimica Acta Part A*, 2005. **62**: p. 105-111.
2. Masashi Sonoyama, M.M., Gen Katagiri, Hideyuki Ishida, *Dynamic FT-IR Spectroscopic Studies of Silk Fibroin Films*. *Applied Spectroscopy*, 1997. **51**(4): p. 545-547.
3. P Petrini, C.P., M.C. Tanzi, *Silk fibroin-polyurethane scaffolds for tissue engineering*. *Journal of Materials Science: Materials in Medicine*, 2001. **12**: p. 849-853.
4. Hyoun-Joon Jin, S.V.F., Gregory C. Rutledge, and David L. Kaplan, *Electrospinning Bombyx mori Silk with Poly(ethylene oxide)*. *Biomacromolecules*, 2002. **3**: p. 1233-1239.